

Analysis of CO₂ capture process from flue-gases in combined cycle gas turbine power plant using post-combustion capture technology



Navaneethan Subramanian ^{*}, Paweł Madejski

AGH University of Science and Technology, Faculty of Mechanical Engineering and Robotics, Al. Mickiewicza 30, 30-059, Kraków, Poland

ARTICLE INFO

Handling Editor: Wojciech Stanek

Keywords:

Combined cycle gas turbine
Heat recovery steam generator
Carbon capture and storage
Post-combustion CO₂ capture
Negative CO₂ emission
Syngas

ABSTRACT

Combined cycle gas turbine power plants (CCGTs) are a combined cycle consisting of a gas turbine and a steam turbine to generate electricity. Sometimes CCGTs incorporate cogeneration to produce both heat and power. After the gas fuel combustion in the gas turbine combustion chamber, the flue gases are passed through the Heat Recovery Steam Generator (HRSG) to extract heat and generate additional electrical power using the steam turbine. The CCGT technology is recognized for its highest efficiency of 58% in electricity production among the power production technology. A highly efficient CCGT power plant with 60% efficiency produces even 2.5 times less CO₂ than a modern coal power plant with an efficiency of 45% because of the use of gas fuel and electrical efficiency. The CO₂ emission can be reduced further when the post-combustion CO₂ capture methods are applied. To perform CO₂ capture and to reduce the CO₂ emission from power plants, the CO₂ mass fraction in flue gas is the crucial parameter for the operation of the Post-combustion Carbon Capture and Storage (PCCS) technology. The PCCS technology uses solvents, which is the aqueous solution of amine that reacts with flue gas and absorbs the CO₂, which is treated and separated later. The paper presents the results of the energy analysis of a post-combustion carbon capture process when integrated with a combined cycle gas power plant. The study considered two different gas fuels such as methane and syngas. Syngas composition was determined from the sewage sludge gasification process and can be treated as zero-emission CO₂ gas fuel. When the flue gas produced from the syngas is used in PCCS at more than 50% of load conditions, the negative CO₂ emission level in large-scale CCGT power plants can be reached. The paper presents the results of mass and energy balance analysis of HRSG of a CCGT integrated with PCCS to perform CO₂ capture. The analysis of HRSG using flue gases from methane and syngas is performed by calculating the enthalpy of flue gas, rate of heat exchange, and temperature distribution of each component of HRSG. The comparison of the result shows slight differences due to the different composition and flow rates of flue gases. The flue gas at the outlet of two HRSG is used in the PCCS at different load conditions. An aqueous solution of 30 wt% Monoethanolamine (MEA) with rich loading of 0.5 mol-CO₂/mol-MEA and a mixture of 16 wt% 2-amino-2-methyl-1-propanol (AMP) – 14 wt% Piperazine (PZ) with rich loading of 0.62 and 0.86 mol-CO₂/mol-amine respectively are used in the PCCS. Due to the reboiler duty of amines, the steam consumed by the PCCS for AMP-PZ regeneration is less compared to MEA. Depending upon the flue gas and solvent used in the PCCS, the power consumed by the PCCS from CCGT power plant is measured from 9.6% to 11.6%. For the given operating condition of the CCGT and PCCS at more than 50% load condition, the negative CO₂ emission level can be achieved.

1. Introduction

The rapid increase in energy demand and the use of fossil fuels to satisfy the demand made the energy sector a large contributor to carbon dioxide (CO₂) emission, the primary gas of greenhouse gases (GHG). Of the total amount of greenhouse gas emissions, about 65% of CO₂ emissions are caused by the power industries. The emission of CO₂ into the

atmosphere is the major cause of global warming [1]. In the United Nations Framework Convention on Climate Change (UNFCCC) Paris agreement, 196 countries assert to maintain the rise of global average temperature below 2 °C [2]. Carbon capture utilization and storage (CCUS) is one method of mitigating CO₂ emission into the atmosphere. The first-generation carbon capture technology had lower CO₂ capture efficiency and difficulties in integrating with existing facilities. With

* Corresponding author.

E-mail address: subraman@agh.edu.pl (N. Subramanian).

more development, the second and third generations overcame such problems. The current generation of carbon capture technology has improved efficiency and cost-effectiveness compared to the previous generation [3]. The captured CO₂ can be utilized in various ways such as in Enhanced Oil Recovery (EOR) for oil and gas recovery during extraction, as a carbonating agent in food products, CO₂ curing in the cement industry, and in the thermochemical conversion process with hydrogen to produce methane [4]. A review by Ref. [5] on various factors of CCUS in hydrocarbon industry, the Technical Readiness Level (TRL) of CCUS, and types of CCS, which indicates the maturity level of the technology. The CCUS has a TRL6, which indicates more investments are needed in CO₂ storage facilities and CO₂ transportation to make CCUS commercially viable by 2030. According to the report by International Energy Agency (IEA) in 2022, 35 commercial CCUS units are currently used for various industrial purposes, which capture up to 45 MtCO₂/year. The further investment in CCUS forecasts that by the year 2030 about 200 CCUS facilities can be established, which will capture 220 MtCO₂/year. The report suggests that retrofitting CCUS to an existing power plant may reduce emission and recovers the investment [6]. The IEA Greenhouse Gas R&D Programme (IEAGHG) report states that it is possible to improve the efficiency of the CO₂ capture rate of the currently used PCCS amine-based technology to 99%, but it increases the cost of equipment and the requirement of energy for amine regeneration. The recent results by Front End Engineering & Design (FEED) show the possibility of deploying a 99% capture rate facility at a cost comparatively 90% capture rate by the year 2030 [7].

The Petra Nova power plant (Thompsons, Texas) and the Boundary Dam (Estevan, Saskatchewan, Canada) are the only commercially established large-scale solvent-based PCCS technology integrated with coal-fired power plants that exist in the power industry [8]. With the Petra Nova power plant suspended operations recently, the Boundary Dam power plant integrated with amine-based carbon capture and storage (CCS) technology is still operational [9]. Both facilities are initially constructed as power plants, and the CCS technology was retrofitted later. While the Boundary dam uses steam from the available steam cycle for amine regeneration, the Petra Nova uses an auxiliary co-generation plant fired with natural gas using a 70 MW GE 7 E A gas turbine, which produced both power and steam for the PCCS plant [10]. The Cansolv amine used in the Boundary Dam power plant is used to capture both carbon dioxide and sulphur dioxide [11]. This amine will also be used in integrating the world's largest carbon capture project with a natural gas-fired combined cycle power plant [12]. The difference between the Petra Nova and the Boundary Dam power plant with CCS is shown in Table 1.

The combined cycle gas turbine power plant (CCGT) has the highest power generation efficiency of more than 60%. At 60% efficiency, the CCGT can produce CO₂ emissions of up to 330 kgCO₂/MWh [13]. Because of their low operational cost, high-power generation efficiency and lower environmental impact, the CCGTs are distinct from other

power generation techniques such as individual power plants with only gas or steam. The utilization of heat from the gas turbine and optimization of HRSG leads the CCPs to improve the power production efficiency up to 65% with a considerable reduction of CO₂ emission [14]. The installation of HRSG at the outlet of the gas turbines not only increases energy efficiency by utilizing the thermal energy in the exhaust gas but also reduces the waste of energy [15]. The gas turbine can change the load rapidly by modifying the fuel mass flow rate according to the demand [16,17].

The IEA report on Bioenergy with carbon capture and storage (BECCS) states that the combining of bioenergy with CCS is a potential solution for achieving a negative emission. Bioenergy involves the production of power and heat from biomass, which originates from agricultural residues and wastes [18]. When biomass is combined with carbon capture, it provides the possibility of achieving negative CO₂ emissions [19]. In 2019, more than 7.5 million tons of sewage sludge were produced by the European Union countries [20]. Vishwajeet et al. experimentally demonstrated the process of converting sewage sludge into syngas using a plasma gasification experimental rig. The gasification took place in two-step plasma gasification, in which the ash produced during the gasification process is involved in the vitrification process, which turned the residue into construction material. The experimental result shows that the use of plasma for gasification influences the heating value of the producer gas. The 2-step process led the experiment to achieve the end-to-waste status and made the waste useful for energy production [21]. Ziolkowski et al. demonstrate the potential of achieving 'negative CO₂ emission gas power plant' with the use of gas fuel produced from the gasification of biomass in a gas power plant integrated with CCS using different modelling software such as Aspen Plus, Aspen Hysys and Epsilon. The comparison of calculation of various parameters such as pressure, temperature, mass flow rate and composition of streams of the cycle from the software show slight differences and possibility of achieving a negative CO₂ emission of -720 kgCO₂/MWh. The Epsilon Professional® software uses the Gauss-Seidel method to perform calculations and uses components to produce mass and energy balance results of the designed thermodynamic cycles [22].

The CCS is performed in three different methods: precombustion carbon capture, post-combustion carbon capture, and oxy-combustion carbon capture. Depending upon the type of CCS, the energy penalty of the power plant varies from 4% to 12%. The post-combustion carbon capture and storage (PCCS) technology using solvent achieves a high CO₂ capture efficiency of 90% and has the advantage of integrating with the complex structure of an existing or new power plant with multiple systems and interconnections of streams [23]. In PCCS using the solvent method, the solvent uses the chemical absorption, in which the liquid solvent reacts with the CO₂ in the gas stream [24]. Diethanolamine (DEA), methyl diethanolamine (MDEA) and Monoethanolamine (MEA) are some of the solvents used in the PCCS process. MEA is the most known solvent for its high rate of reaction, low cost, and CO₂ absorption capacity [25]. The use of solvent method for CO₂ capture requires high energy for solvent regeneration, which depends upon the type of solvent used [26]. Recent research focuses on high CO₂ capture rate with low requirement of energy for regeneration. This condition works especially with blending of amines [27]. Sakwattanapong et al. conducted a bench-scale experimental analysis that shows that the reboiler duty required for single alkanolamine is higher and for blended amines is the combination of the two single amines used or lower than one of the amines used in the blended solutions. The reboiler duty required for MEA and MDEA at rich loading of 0.5 mol/mol and lean loading of 0.30 mol/mol and 0.5 mol/mol is around 3500 kJ/kg-CO₂ and 1500 kJ/kg-CO₂ respectively. In case of the 1:1 M ratio of MEA-MDEA blended amines at rich loading of 0.5 mol/mol and lean loading of 0.15 mol/mol, the required reboiler duty is around 2000 kJ/kg-CO₂, which is the combination of both amines used or lower than MEA. The reboiler duty also depends upon various factors such as amine concentration, and rich and lean loading [28]. Śpiewak et al. used a process

Table 1
Comparison between the Petra Nova and Boundary Dam power plant with CCS [10].

Parameter	Unit	Petra Nova Power Plant	Boundary Dam power plant
Location	–	Thompsons, Texas	Saskatchewan, Canada
Gross power generation	MW	240	160
CO ₂ captured	MT/year	1.6	1
Capture efficiency	%	90	90
Regeneration steam	–	Auxiliary co-generation plant	Steam cycle
Solvent	–	KS-1	Cansolv
Use of captured CO ₂	–	Enhanced Oil Recovery	also to geological storage
Capital cost	\$	1000	1300–1500

development unit and compared the performance of the solvents MEA and 2-amino-2-methyl-1-propanol (AMP) mixed with piperazine (PZ). It shows that the process efficiency of using AMP-PZ solvent is similar to MEA. However, the heat required for the regeneration process is lower for AMP/PZ than for MEA with similar carbon capture efficiency [29]. A model developed for the study of PCCS using AMP-PZ and MEA solvents integrated with a supercritical coal power plant shows that the reboiler duty required for the regeneration of AMP-PZ is lower than MEA, which is 2.9 GJ/t-CO₂ and 3.6 GJ/t-CO₂ respectively. The power and cooling water consumed by PCCS using AMP-PZ is lesser than MEA. However, due to the volatility of AMP-PZ, the emission of the amine into the atmosphere is high at 18 g/t-CO₂ [30].

While using solvents in PCCS, emission of amine and ammonia with treated flue gas and captured CO₂ can be observed. The amine emission depends on many factors such as operating conditions of PCCS, flue gas composition and temperature of the solvent, which leads to various environmental issues. The emission of amine can be partly reduced by adding a water wash column to the top of the absorber, which reduces the temperature of the flue gas. This does not have much effect on ammonia emission [31]. A pilot plant experimental investigation on amine degradation management using blended AMP-PZ states that the recirculating solvents used in the PCCS consist of anionic compounds, metals, and reactive components. The experiment states that the corrosivity in MEA is higher than in the mixture of AMP-PZ. After the same number of days of operation, the iron accumulation in MEA and AMP-PZ are measured to be 63 mg/kg and 3 mg/kg respectively [32].

In this study, thermodynamic analysis of flue gases obtained from two different fuels, the water/steam circuit of the components in HRSG, the performance of HRSG in CCGT, and the theoretical analysis of PCCS using two different solvents integrated with the CCGT are presented. The results of the analysis of flue gas properties, emission from flue gases, energy balance, and heat distribution of the components of HRSG are presented. This study's novelty is to analyze the post-combustion carbon capture and storage using two different solvents such as MEA and a mixture of AMP-PZ. Two different fuels such as methane and syngas obtained from the gasification of sewage sludge are used in the gas turbine. The exhaust of the gas turbine is used in HRSG of the CCGT and further passed to PCCS. The analysis of flue gases from the CCGT is treated with PCCS under different load conditions (100%, 75%, 50% and 25%) are performed. An aqueous solution of 30% MEA with rich CO₂

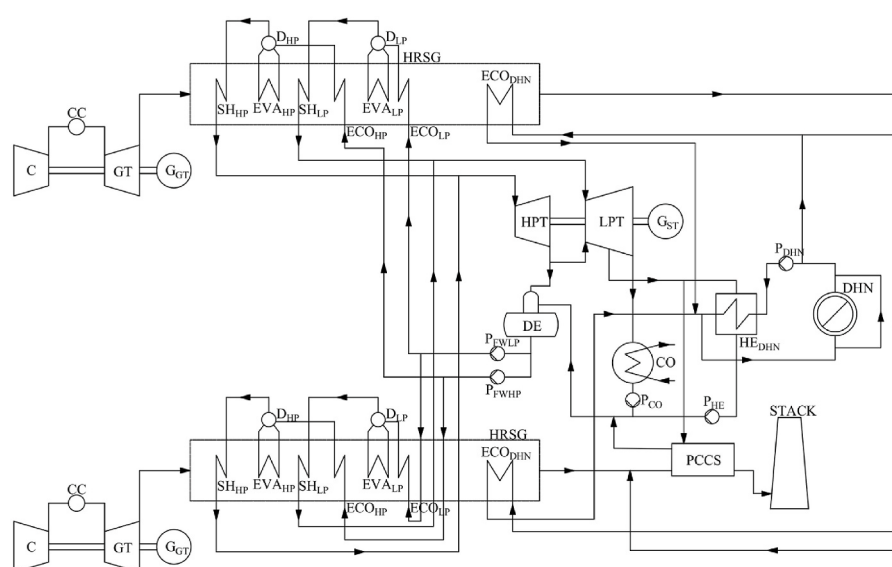
loading of 0.5 mol-CO₂/mol-MEA and 16% AMP +14% PZ with rich CO₂ loading of 0.62 and 0.86 mol-CO₂/mol-amine respectively are used in the PCCS. The various parameters of each stream, steam and power consumption of the PCCS are analyzed using different solvents for treating flue gases from different fuels.

2. General scheme and description of analyzed CCGT

To perform an analysis of the HRSG of the CCGT, the Gorzów CCGT power plant in Poland is taken as a reference case [33]. Fig. 1 shows the overall layout of the CCGT integrated with PCCS power plant taken into consideration for the analysis with reference to the Gorzów power plant. The CCGT used for the thermodynamic analysis of HRSG consists of two gas turbines, two HRSG, and a steam turbine. The fuel and air mixture gets combusted in the combustion chamber, and the flue gas at 30 bar pressure and 1410 °C temperature flows through the gas turbine, which produces power at an efficiency of 38.3%. The exhaust of the gas turbine passes through the HRSG and converts the water inside the tubes of HRSG into steam. The steam produced from the HRSG is further sent to the steam turbine. Part of the steam is extracted from the steam turbine for the District Heating Network (DHN) and PCCS for solvent regeneration. Before passing the flue gas to PCCS, the sensible heat in flue gas is utilized by the DHN economizer at the last stage of the HRSG. The considered CCGT power plant consists of 2 SGT-800 gas turbines (properties in Table 2), which can produce power up to 50.5 MW separately, and the Siemens SGT-400 steam turbine (properties in

Table 2
Properties of siemens SGT-800 [34].

Parameter	Unit	Value
Power generation	MW	ISO 50.5
Electrical efficiency	%	38.3
Frequency	Hz	50
Heat rate	kJ/kWh	9407
Speed	rpm	6608
NOx emission	ppmV	<15
Gas-supply pressure requirement	bar	27–30
Compressor pressure ratio	–	21.1:1
Exhaust gas temperature	°C	553



C - Compressor, CC - Combustion Chamber, CO - Condenser, DE - Deaerator, DHN - District Heat Network, DHP - High Pressure Steam Drum, DLP - Low Pressure Steam Drum, ECO - Economizer, EVA - Evaporator, FWP - Feed water pump, G - Generator, GT - Gas Turbine, HE - Heat Exchanger, HP - High Pressure, HPT - High Pressure Turbine, HRSG - Heat Recovery Steam Generator, LP - Low Pressure, LPT - Low Pressure Turbine, P - Pump, SH - Superheater, ST - Steam Turbine, PCCS - Post-combustion Carbon Capture and Storage

Fig. 1. Schematic diagram of combined cycle gas turbine power plant integrated with post-combustion carbon capture technology using solvent method.

Table 3
Properties of SST 400 steam turbine [35].

Parameter	Unit	Value
Power Output	MW	Up to 65
Frequency	Hz	50
Speed	rpm	3000–8000
Live Steam Temperature	°C	540
Live Steam Pressure	bar	Up to 140
Reheat Steam Temperature	°C	Up to 450
Reheat Steam Pressure	bar	Up to 30
Turbine extraction steam pressure	bar	Up to 60
Exhaust steam conditions		
Back pressure		Up to 25 bar
District heating		Up to 3 bar
Condensing		Up to 0.6 bar
Mechanical efficiency	%	99.6
Generator efficiency	%	98.5
HP & LP Isentropic efficiency	%	92 & 88

Table 3) produces power up to 65 MW. The mass flow rate and the composition of flue gases passing through the HRSG vary depending on the fuels used. The detailed information about the HRSG used for the analysis is described in section 3.

3. Description of HRSG and PCCS using solvents

3.1. Heat recovery steam generator – arrangement and operation principle

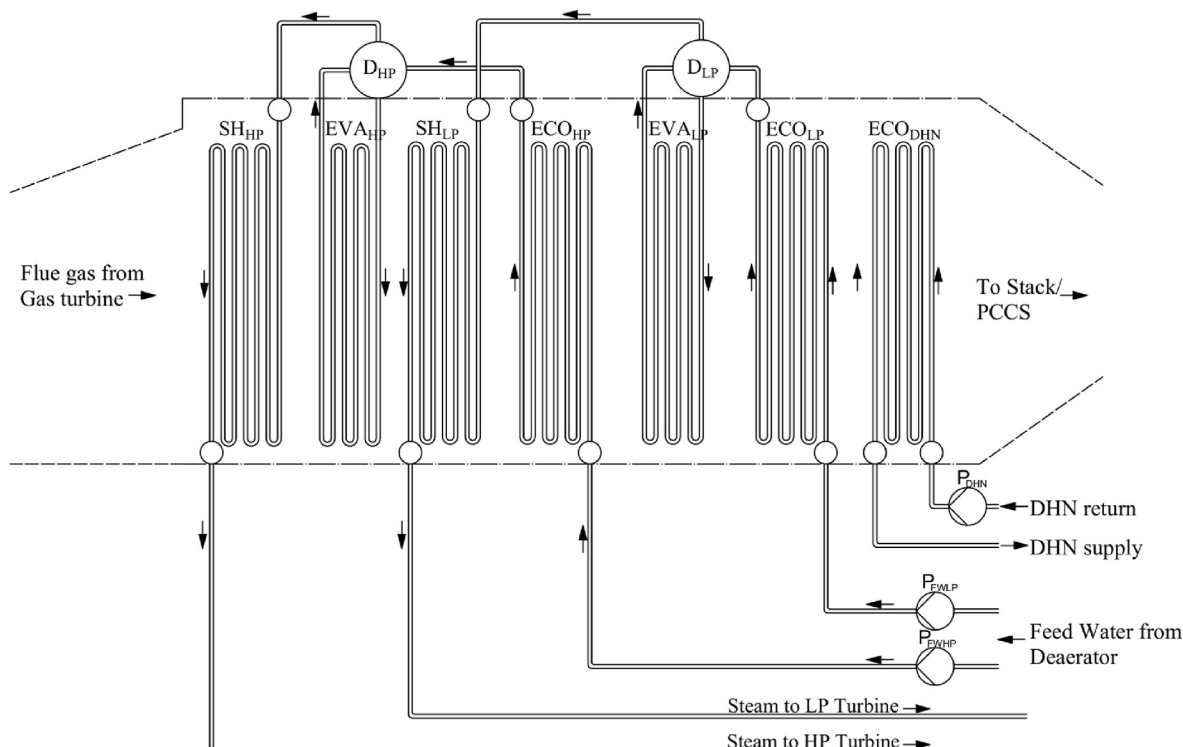
Fig. 2 shows the detailed arrangements of the components of HRSG used for the analysis. The HRSG consists of two pressure levels such as high pressure (HP) and low pressure (LP) as the values of the pressure levels are indicated in Table 6. Each pressure level has its economizer, evaporator, steam drum and superheater. The increasing number of pressure levels in HRSG improves the efficiency of the power plant. The increasing pressure levels extract more heat from flue gas, which

produces more steam for steam turbines for power generation. The utilization of heat until the reduction of the temperature difference between flue gas and steam enhances the efficiency of HRSG [36]. Since the flue gas stream at the final stage of the HRSG attains a temperature of 178 °C, adding one more pressure level is not viable, as the temperature difference between the flue gas and steam attains is near 15 °C. Furthermore, the available heat in flue gas is used by the economizer of the DHN, which is included at the last stage of the HRSG.

Water from the deaerator pumped by the HP and LP Feed Water Pumps (FWP) to the economizer gets preheated by the flue gas. The heat to the components of the HRSG is provided by the exhaust gas from gas turbine at 553 °C passing through the duct. The pre-heated stream from economizer flows to the drum, where the separation of water and steam takes place at the separator. The separated steam becomes superheated steam in the superheater and flows to the steam turbine [37]. The water flows the downstream of evaporator and the steam flows through the superheater tubes as described in Fig. 3. Table 4 shows the specifications of the pump, deaerator, and the components of the HRSG used for the analysis.

3.2. Post-combustion carbon capture and storage process

As in Fig. 4, the PCCS includes an absorber and a stripper, where absorption and desorption processes take place. The amine passes through the middle of the absorber and reacts with the flue gas stream passing from the bottom. An exothermic reaction occurs between the flue gas and amine, increasing the temperature of the rich amine from 40 °C to 60 °C streaming out of the absorber bottom. The amine passing through one section of the stripper gets heated to 120 °C, which is the operating temperature of the stripper and flows to the reboiler. When the amine flows back to another section of the stripper, it separates the CO₂ and vapour. Initially, the flue gas and lean amine are cooled down to the operating temperature of 40–60 °C before passing to the absorber.



D - Steam drum, ECO - Economizer, EVA - Evaporator, FWP - Feed water pump, HP - High Pressure, LP - Low Pressure, P - Pump, SH - Superheater, DHN - District Heating Network

Fig. 2. Detailed arrangement of Heat Recovery Steam Generator with two pressure levels.

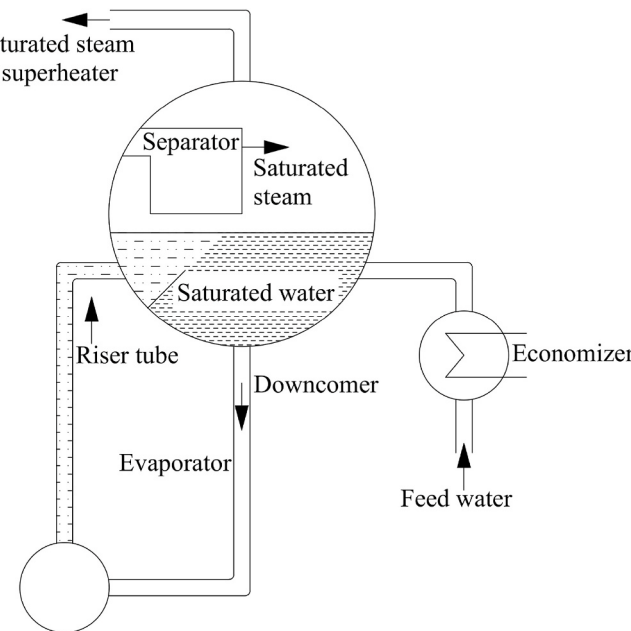


Fig. 3. Water and steam separation process inside steam drum.

Table 4
Specifications of components and equipment of HRSG.

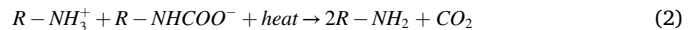
Specifications	Unit	Value
HRSG components flue gas pressure drop	bar	0.2
HRSG HP & LP components cold side heat transfer coefficient	W/m ² K	500
HRSG HP & LP components hot side heat transfer coefficient	W/m ² K	50
Operating pressure of deaerator	bar	7
HP & LP Feedwater pump mechanical efficiency	%	99.8
HP & LP Feedwater pump isentropic efficiency	%	80
HP & LP Feedwater pump speed	rpm	3000
HP & LP Feedwater pump motor mechanical efficiency	%	99.8
HP & LP Feedwater pump motor electrical efficiency	%	85

Water wash is performed on the treated flue gas to reduce the amine and amine emission loss into the atmosphere. Steam at a temperature of 100–140 °C and pressure of 1 bar–3.5 bar is used in the reboiler for heating purposes. While the regenerated lean amine is further used for repeating the process, the separated CO₂ is sent to storage [38–41]. For the analysis of PCCS at different load conditions, the PCCS is intended in a way that the CCGT performs in full operating condition, only flue gas at the exhaust of the CCGT is diverted to PCCS for CO₂ removal. During different load conditions, the remaining flue gas diverted from PCCS is passed directly into the atmosphere.

In this study, two different solvents as MEA and AMP-PZ mixture, are used in the PCCS process. The amine in reaction Eq. (1) is denoted as R, where the amine reacts with CO₂ to form carbamate [42].



The carbamate nitrogen-carbon bond can be broken by the application of heat, which produces a reverse reaction Eq. (2) to form amine regeneration.



As per reaction Eq. (1), the amine reacts with CO₂ and produces carbamate in the absorber. Reaction Eq. (1) is reversed in reaction Eq. (2) in stripper, where heat is used to separate CO₂ from amine. 2 mol of amine react with 1 mol of CO₂ in reaction Eq. (1), in which the CO₂ is separated in reaction Eq. (2) and limit the absorbing capacity of the amine to 0.5 mol (22 g) of CO₂ per mole of amine. The lean solvent used for the carbon capture process in the absorber has a composition of 30 wt% MEA and 70 wt% H₂O, which gives 90% of CO₂ capture efficiency [43]. The Reboiler duty required for the regeneration of MEA is 3.8 MJ/kg-CO₂ [44]. After the regeneration process, the lean solvent at the outlet of the stripper has some content of CO₂, which is represented as lean loading. The lean CO₂ loading for MEA aqueous solution used for the analysis is 0.17 mol CO₂/mol MEA [45]. Converting the mole CO₂ loading of MEA into mass, it is assessed that the CO₂-rich loading of MEA solvent is 0.36 kg-CO₂/kg-MEA.

In case of AMP-PZ, the rich CO₂ loading for AMP and PZ are 0.62 and 0.86 mol-CO₂/mol-amine, respectively [46]. The CO₂-rich loading of AMP-PZ is calculated to be 306 g CO₂/kg AMP and 439 g CO₂/kg PZ. The AMP & PZ has an optimal lean loading of 0.37 mol-CO₂/mol-AMP [47] and 0.20 mol-CO₂/mol-PZ [48]. To compare with MEA and get 90% of CO₂ capture efficiency, 16 wt% AMP and 14 wt% PZ amine mixture are considered for the analysis. The regeneration energy required for 30 wt % AMP-PZ mixture is given by 3.7 MJ/kg-CO₂ [49].

4. Thermodynamic analysis of reference case for modern CCGT

4.1. Main assumptions and properties of fuels

Two different fuels, such as methane and syngas produced from the gasification of sewage sludge with properties as in Table 5 are considered for the analysis. The main assumptions of input data of the HRSG are based on the gas turbine and steam turbine properties in Table 2, Table 3, and Gorzów CCGT power plant [33] to analyze the heat distribution and the properties of flue gas at various stages of HRSG as in Table 6.

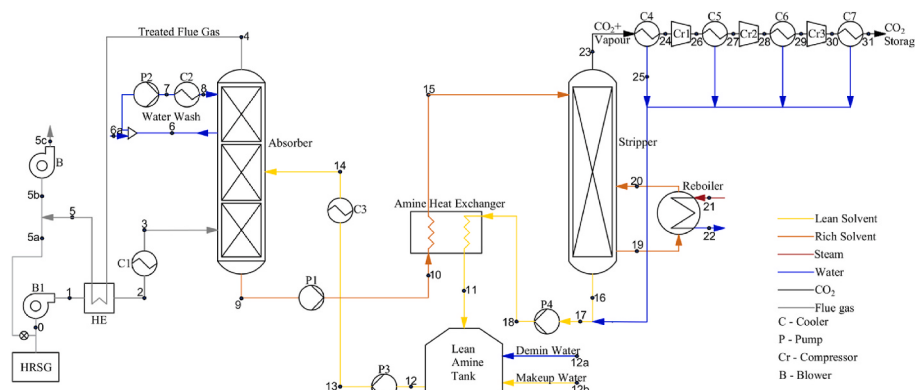


Fig. 4. Post-combustion carbon capture and storage technology using solvent method with reference points.

Table 5
Properties of methane and syngas fuels.

Component	Molecular formula	Unit	Methane		Syngas	
			Mass fraction	Volumetric fraction	Mass fraction	Volumetric fraction
Carbon Monoxide	CO	%	–	–	13.31	9.09
Carbon Dioxide	CO ₂	%	–	–	59.31	25.61
Methane	CH ₄	%	100	100	11.46	13.64
Propane	C ₃ H ₈	%	–	–	8.03	3.39
Hydrogen	H ₂	%	–	–	5.10	45.16
Ammonia	NH ₃	%	–	–	2.79	3.10
Total	–	%	100	100	100	100
Fuel mass flow rate in GT	–	kg/s	2.64	–	7.572	–
LHV ^a	–	MJ/kg	50.70	–	17.079	–

^a LHV based on ISO 6976:1995(E) at 15 °C and 1 atm for gas mixtures.

Table 6
Input data of one HRSG of combined cycle power plant.

Parameter	Unit	Value
HRSG to HP/LP ST steam pressure	bar	80/8
HRSG to HP/LP ST steam temperature	°C	510/
		277
Mass flow of steam to HP steam turbine	t/h	62.4
Mass flow of steam to LP steam turbine	t/h	15.0
Thermal capacity in steam (thermal output)	MW _t	67
Thermal capacity ECO _{DHN} (DHN - thermal output of hot water)	MW _t	10
DHN supply temperature	°C	90

4.2. Thermodynamic analysis of HRSG

The enthalpy of flue gas at different temperatures using different fuels in HRSG is calculated by Eq. (3).

$$h_{fg@t} = \sum_i^N X_i \bullet h_i \quad (3)$$

Where X_i is the mass fraction of the selected gas component in flue gas and h_i is the enthalpy of the selected gas component at the target temperature of flue gas.

The Logarithmic Mean Temperature Difference (LMTD) to determine the temperature driving force of the components in HRSG is calculated as presented in Eq. (4).

$$LMTD = \frac{\Delta T_A - \Delta T_B}{\ln\left(\frac{\Delta T_A}{\Delta T_B}\right)} \quad (4)$$

$$\Delta T_A = T_{hi} - T_{co} \quad (5)$$

$$\Delta T_B = T_{ho} - T_{ci} \quad (6)$$

Where T_{hi} & T_{ho} are the temperature of the hot stream inlet and outlet and T_{ci} & T_{co} are the temperature of the cold stream inlet and outlet of the heat exchanger.

The heat exchange equation for calculating the rate of heat exchange in HRSG is presented in Eq. (7).

$$\dot{Q} = \dot{m}_{fg} \bullet (h_{fi} - h_{fo}) = \dot{m}_{steam} \bullet (h_{so} - h_{si}) \quad (7)$$

Where \dot{m}_{fg} & \dot{m}_{steam} are the mass flow of flue gas and steam, h_{fi} & h_{fo} are the enthalpy of the flue gas at the inlet and outlet of the heat exchanger and h_{so} & h_{si} are the enthalpy of steam at the inlet and outlet of the heat exchanger.

4.3. Analysis of post-combustion carbon capture and storage unit

The reference points are provided at each stream of the post-combustion carbon capture process, as depicted in Fig. 4, to calculate the mass balance of the streams in PCCS. The utilities of the PCCS

process, such as pumps, heat exchangers, coolers, and compressors/blowers, are simulated in Epsilon Professional® 16.00 to calculate the power consumed, heat exchange rate, and outlet stream temperature.

The amount of solvent required for the CO₂ capture process is calculated by the formula presented in Eq. (8).

$$\dot{m}_{14} = \dot{m}_{fg,CO_2} \bullet mg_{amine} \quad (8)$$

Where \dot{m}_{fg,CO_2} is the mass flow rate of CO₂ in the flue gas and mg_{amine} is the rich CO₂ loading of amine in kg/kg. Since the solvents have a carbon capture efficiency of 90%, Eq. (9) shows the mass flow of CO₂ captured at the absorber.

$$\dot{m}_{cap,CO_2} = 0.9 * \dot{m}_{fg,CO_2} \quad (9)$$

The \dot{m}_3 is represented as the total mass flow rate of flue gas used at the inlet of the PCCS absorber. The treated flue gas from PCCS, which is the flue gas after the removal of CO₂ content, is calculated by Eq. (10).

$$\dot{m}_4 = \dot{m}_3 - \dot{m}_{cap,CO_2} \quad (10)$$

The mass flow of rich amine, \dot{m}_9 at the outlet of the absorber and the inlet of the stripper is given in Eq. (11)

$$\dot{m}_9 = \dot{m}_{14} + \dot{m}_{cap,CO_2} \quad (11)$$

Here \dot{m}_{14} is the mass flow of lean amine at the absorber inlet. The inlet and outlet mass balance of the absorber is given in Eq. (13)

$$\dot{m}_3 + \dot{m}_{14} = \dot{m}_4 + \dot{m}_9 \quad (13)$$

The mass flow of rich amine at the outlet of the absorber and the inlet of the stripper is denoted as \dot{m}_9 and \dot{m}_{15} respectively. Since the LP steam for PCCS reboiler and DHN are extracted from the same line of steam turbine of CCGT, the steam for both MEA and AMP-PZ regeneration is at 135 °C and 3 bar for all operational conditions. Hence, to calculate the required steam flow, h_{21} is taken as 2728.22 kJ/kg. The reboiler has a steam pressure drop of 0.1 bar, which gives the outlet pressure of 2.9 bar and temperature of 132.37 °C (calculated from saturated steam properties). The enthalpy of water at the outlet of the reboiler h_{22} is taken as 556.6 kJ/kg. The Reboiler duty required for capturing CO₂ is calculated from Eq. (14)

$$\dot{Q}_{21} = \dot{Q}_{amine} * \dot{m}_{cap,CO_2} \quad (14)$$

Where \dot{Q}_{amine} is the reboiler duty of the amine. The energy rate of the LP steam supplied for the process in the reboiler is given in Eq. (15)

$$\dot{Q}_{21} = \dot{m}_{lpsteam} \bullet (h_{21} - h_{22}) \quad (15)$$

Where h_{21} & h_{22} are the enthalpy of steam at the reboiler inlet and outlet. To calculate the mass flow of steam to reboiler required for the regeneration of amine Eq. (15) is written as Eq. (16)

$$\dot{m}_{lpsteam} = \frac{\dot{Q}_{21}}{(h_{21} - h_{22})} \quad (16)$$

The separated CO₂ from amine after regeneration process passing through the top of the stripper at point 23 consists of 10% of H₂O from the rich amine. The mass flow of vapour is given in Eq. (17)

$$\dot{m}_{\text{vapour}} = 10\% \bullet \dot{m}_{15} \quad (17)$$

When using 30% aqueous amine solution, water impurities are present at the final stage of the capture process. The CO₂ at a purity of 99.8 (vol%) can be captured using the PCCS process [50]. Based on the CO₂ purity, a 0.2% loss of H₂O content in amine during the regeneration and CO₂ storage process is assumed. The mass flow rate of lean solvent at the outlet of the stripper is given in Eq. (18)

$$\dot{m}_{17} = \dot{m}_{15} - \dot{m}_{\text{cap.CO}_2} - 0.2\% \bullet \dot{m}_{\text{vapour}} \quad (18)$$

After the regeneration process, the mass flow of vapour escaped with the captured CO₂ at the outlet of the stripper is assumed to be 10%. The mass flow rate of captured CO₂ with vapour is given in Eq. (19)

$$\dot{m}_{23} = \dot{m}_{\text{cap.CO}_2} + \dot{m}_{\text{vapour}} \quad (19)$$

After the PCCS process, the CO₂ is compressed and cooled at multi-stage until it achieves 110 bar pressure for storage. The temperature and pressure at each balance point are given with reference to the literature [51–56]. The mass flow rate of CO₂ sent to storage is given by Eq. (20)

$$\dot{m}_{31} = \dot{m}_{23} - 99.98\% \bullet \dot{m}_{\text{vapour}} \quad (20)$$

The flue gas outlet from HRSG is given as input to the PCCS process. Based on the operational conditions of PCCS in section 3.2 and the design of PCCS, the initial input of the PCCS analysis is shown in Table 7.

5. Results of thermodynamic analysis

5.1. Performance of HRSG using flue gases from different fuels

The thermodynamic analysis of flue gas and steam passing through each stage of the HRSG components is performed using the reference points provided at each stream of the HRSG as in Fig. 5. The properties are calculated using flue gas obtained from methane and syngas. Based on the thermodynamic analysis of gas turbine, depending upon the mass flow of fuel required for power generation and the LHV of the fuels, the mass flow of flue gases obtained from the combustion of gas fuels in one gas turbine using methane and syngas fuels are 133.89 kg/s and 133.52 kg/s respectively.

5.1.1. Flue gas analysis

When using different gas fuels in the SGT-800 gas turbine, the turbine increases the mass flow of fuel according to the power generation requirement and the exhaust gas is kept at a constant temperature. In this analysis, the gas turbine produces 50.5 MW of power with the mass flow of methane and syngas at 2.64 kg/s and 7.572 kg/s respectively. The exhaust gas at 553 °C and pressure of 1.02 bar was produced using

Table 7
Input data for PCCS analysis.

Parameters	Unit	Value
Absorber operating temperature	°C	40
Absorber operating pressure	bar	1
Absorber pressure drop	bar	0.1
Stripper operating temperature	°C	120
Stripper operating pressure	bar	2
Stripper pressure drop	bar	0.5
Steam temperature to reboiler	°C	135
Steam pressure to reboiler	bar	3
Coolers pressure drop	bar	0.05
Cooling water temperature	°C	15
CO ₂ capture efficiency	%	90
CO ₂ to storage temperature	°C	<30 °C
CO ₂ to storage pressure	bar	110

the fuels. The methane and syngas composition as in Table 5 is used in the gas turbine model at 30 °C and 25 bar to calculate the composition of exhaust gas produced as in Table 8.

5.1.2. Calculation results of enthalpy of flue gas

Using the flue gas from methane and syngas use, the flue gas temperature at the inlet and outlet of the components of the HRSG is computed, and with the use of Eq. (3) the enthalpy of flue gas is calculated too. The flue gas content in Table 8, enthalpy of gas content [57,58] and the calculated temperature difference in HRSG are taken into consideration for the calculation. For a better understanding of heat distribution in HRSG, the calculated enthalpy and temperature of flue gas from methane and syngas are plotted in Figs. 6 and 7 respectively with reference to the components and the reference points of HRSG as shown in Fig. 5.

The enthalpy of flue gases at various stages of HRSG from methane and syngas fuels appears nearly the same. When comparing the composition of flue gases from methane and syngas from Table 8, the major differences in proportions are observed only in N₂ and CO₂ content, and the other gas proportions are quite similar to each other. The methane flue gas has high N₂ and low CO₂ content than syngas flue gas. When calculating the total enthalpy, the low N₂ and high CO₂ content in flue gas from syngas gets compromised, which makes the enthalpy value of flue gases from both fuels at various points of HRSG similar.

5.1.3. Heat distribution in HRSG

The calculated flue gas enthalpy at various stages of HRSG and the input of HRSG is used in Eq. (7) to calculate the steam/water enthalpy at the inlet of the component. With reference to the enthalpy of steam/water, the temperature of the HP steam, LP steam and DHN are calculated. The calculated temperature is plotted in Figs. 8 and 9 for flue gas passing through HRSG from methane and syngas fuels respectively with reference to the components and reference points of HRSG as in Fig. 5. Even though the temperature of the flue gas at HRSG for both flue gases are same, due to the different mass flow rate flue gas, the steam/water temperature varies. In both cases, the final temperature of HP and LP steam is kept constant at 510 °C and 277 °C respectively. In order to achieve the final steam temperature, the pressure drop of the components of HRSG in both the hot and cold sides is kept the same for both flue gases. Due to the constant steam temperature and pressure drop of the components, a slight difference in water/steam temperature is observed under varying flue gas mass flow rates from different fuels.

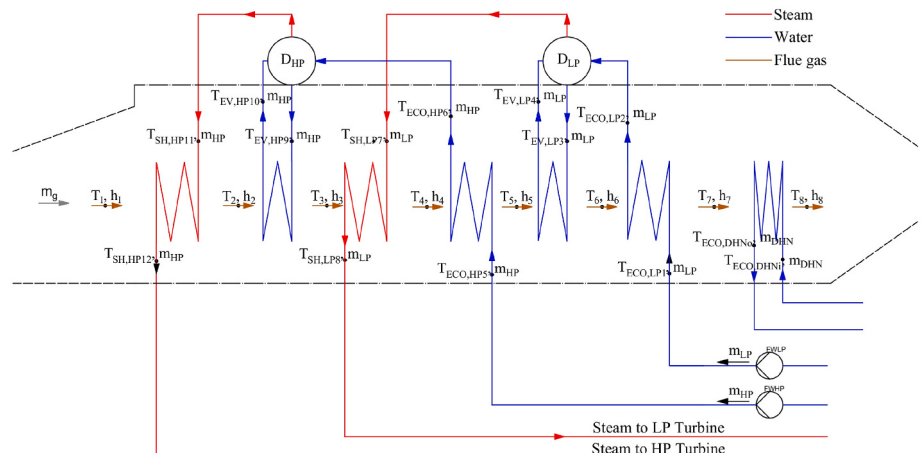
5.1.4. Calculation of LMTD and rate of heat exchange

With the calculated enthalpy of flue gas and steam temperature, using equations (4)–(7) the LMTD and the rate of heat exchange of the components in HRSG are calculated as shown in Table 9 and Fig. 10 respectively with reference to Fig. 5. As observed from the calculated enthalpy and heat distribution of flue gases in HRSG, the content, mass flow rate and enthalpy of flue gas vary according to the type of fuel used, which has an impact on the change in performance of the component of HRSG.

When referring to the calculated LMTD in Fig. 5, it can be seen that the LMTD is high in the HP superheater, HP evaporator, LP superheater and DHN at the range of 11.5 MW, 26.1 MW, 9.3 MW and 9.31 MW respectively for flue gases from both fuels. This is due to the high-temperature difference between the steam and flue gas passing through the components. Since the economizers are used majorly for preheating, it has a low LMTD of 0.99 MW and 0.03 MW for HP and LP pressure levels respectively. It can be noted from Fig. 10, the heat exchange rate using flue gases from both fuels is nearly the same. In both HP and LP, a high rate of heat exchange takes place at the evaporators.

5.2. Results and analysis of post-combustion carbon capture process

The calculations performed for HRSG are for one HRSG in the CCGT.



T - Temperature, m - mass flow rate, h - enthalpy, g - flue gas, FW - Feedwater pump, D - steam drum, HP - High Pressure, LP - Low Pressure, SH - Superheater, EV - Evaporator, ECO - Economizer, DHN - District Heating Network

Fig. 5. Flue gas path and water/steam line of HRSG components with reference points.

Table 8

Detailed composition of the exhaust gas from the SGT-800 turbine determined with Epsilon Professional® 16.00 (10 ppmv dry level, 15% O₂).

Component	Composition of the exhaust gas [%]			
	Methane		Syngas	
	Mass	Molar	Mass	Molar
N ₂	74.3274	75.1939	71.6727	72.8608
O ₂	14.7585	13.0711	14.6017	12.9949
Ar	0.4314	0.3059	0.4152	0.296
H ₂ O	5.0355	7.9213	5.6072	8.8637
CO ₂	5.4456	3.5067	7.7016	4.9836
NO _x	0.0016	0.0011	0.0016	0.001

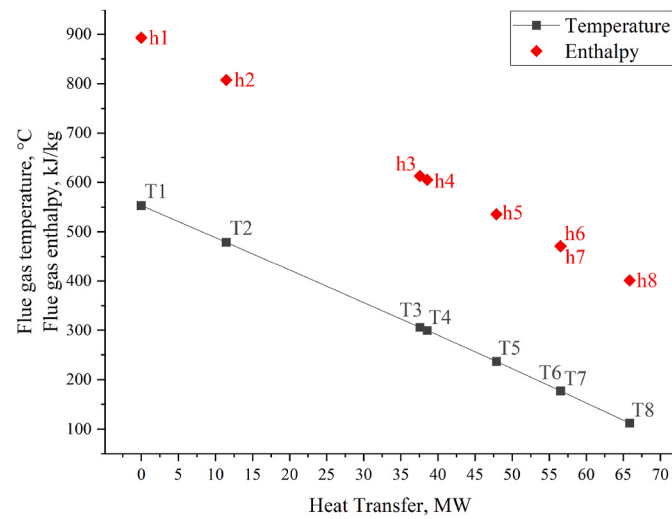


Fig. 6. Enthalpy of flue gas from methane at the inlet and outlet of the components of HRSG.

Since the CCGT power plant considered for analysis has two HRSGs, the total exhaust gas mass flow rate from the HRSG to PCCS with flue gases from methane and syngas fuels are 267.78 kg/s and 267.04 kg/s respectively. The mass flow rate of flue gases from two HRSG is considered for the analysis in PCCS using two different solvents MEA and a mixture of AMP-PZ. From the total mass flow rate of flue gas and emission analysis of flue gas from gas turbines in Table 8, the mass flow

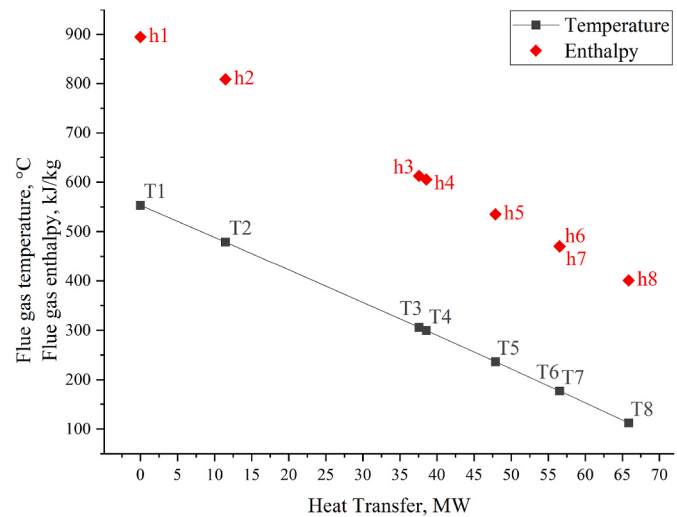


Fig. 7. Enthalpy of flue gas from syngas at the inlet and outlet of the components of HRSG.

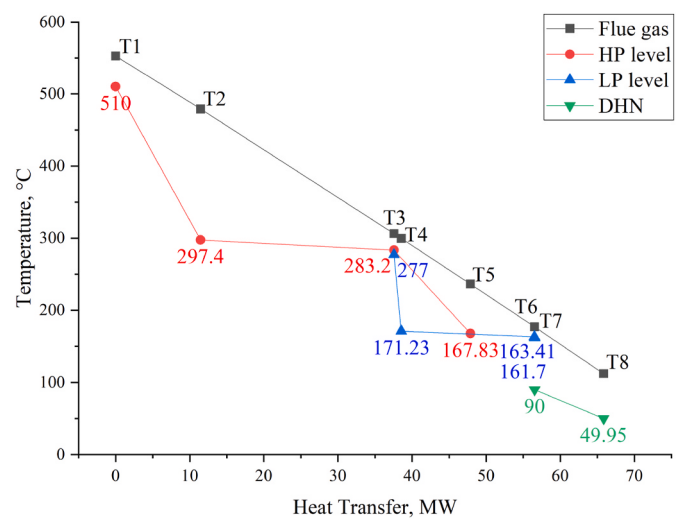


Fig. 8. Heat distribution in HRSG using flue gas from methane fuel.

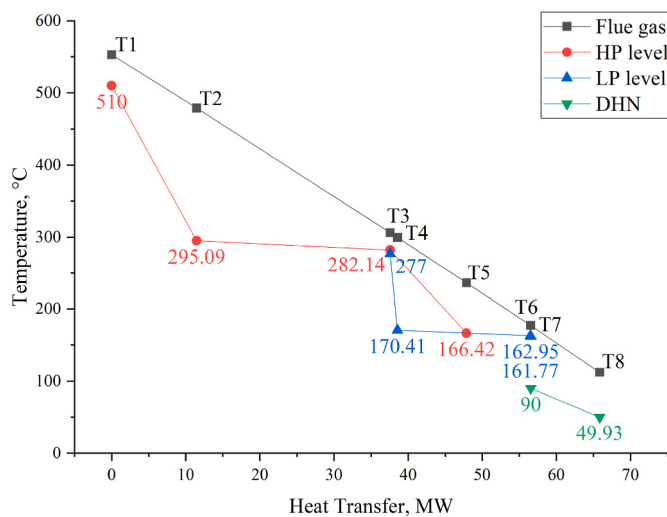


Fig. 9. Heat distribution in HRSG using flue gas from syngas fuel.

Table 9
LMTD values of the components of HRSG.

HRSG components	LMTD (°C)	
	Methane fuel	Syngas fuel
HP SH	96.8	97
HP EVP	76.9	78.7
LP SH	67.3	67.3
HP ECO	36.5	37.8
LP EVA	33.02	33.7
LP ECO	14.45	14.65
DHN	73.89	73.9

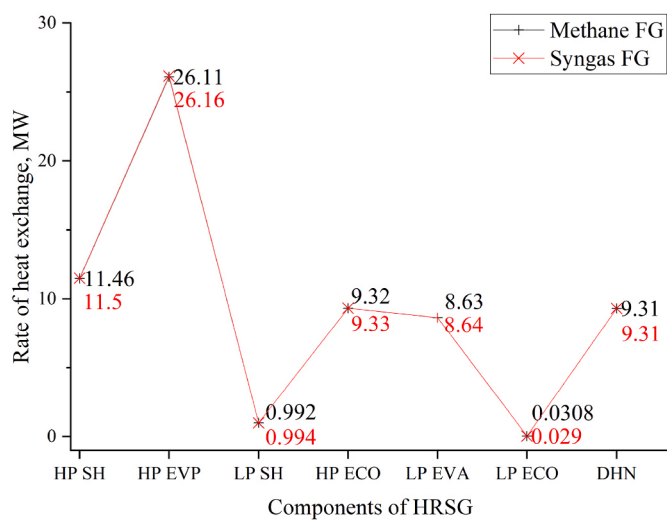


Fig. 10. Rate of heat exchange of each component of HRSG.

rate of CO₂ produced from methane and syngas is calculated to be 14.73 kg/s and 20.56 kg/s, respectively.

The flue gas from CCGT at the inlet of PCCS is reduced under different load conditions such as 75%, 50%, and 25% to analyze the behavior of the PCCS process. In these load conditions, the flue gas diverted from PCCS is passed into the atmosphere. When analyzing the utilities of PCCS such as blowers, pumps and compressors using simulation, the outlet temperature and pressure of the stream remain the same, but the mass flow rate of the streams varies at different flue gas load conditions. At different load conditions, the increase in CO₂ in flue

gas increases the required mass flow rate of solvent, mass flow rate of steam required for reboiler and capture rate of CO₂ according to the requirement. This varies the stream flow rate in PCCS depending upon the CO₂ content in the flue gas.

5.2.1. Results of PCCS process using MEA solvent

The mass flow rate of each stream of the PCCS technology is calculated using Eq. (8) to Eq. (16). As per the rich CO₂ loading of MEA taken into consideration for the analysis, 1 kg-MEA is required to absorb 0.36 kg-CO₂. With reference to the rich CO₂ loading and using Eq. (8), the required mass flow rate of lean MEA solvent to treat 14.73 kg/s and 20.56 kg/s of CO₂ in flue gases from methane and syngas fuel in PCCS process is calculated to be 136.27 kg/s and 190.25 kg/s respectively. At the outlet of the stripper, the solvent consists of a small proportion of CO₂ which cannot be completely removed, which is the lean loading of MEA. As per the lean loading calculation, 5.01 kg-CO₂ and 6.99 kg-CO₂ are present in the total flow rate of 136.27 kg/s and 190.25 kg/s solvent for treating flue gases from methane and syngas respectively. Due to the lean loading, the MEA lean solvent used for the recirculation in the PCCS process consists of 28.4% MEA + 3.68% CO₂ + 67.92% H₂O.

Since the mass flow of flue gas is reduced due to different load conditions, it reduces the CO₂ content in the flue gas as in Table 10 and Table 11. At this condition, the requirement of MEA and steam required for reboiler in PCCS reduces as in Figs. 11–13. The detailed parameters of the reference points of the streams in Fig. 4 of PCCS using MEA are given in Appendix A.

5.2.2. Results of PCCS process using AMP-PZ solvent

Similar to PCCS using MEA, the mass balance of PCCS using AMP-PZ solvent mixture is calculated and the notable parameters are plotted in Figs. 14–16. As per the AMP-PZ rich loading, 0.306 kg-CO₂ and 0.439 kg-CO₂ were absorbed by 1 kg of AMP and 1 kg of PZ respectively. Hence, to treat 14.73 kg/s of CO₂ in flue gases from methane fuel, the mass flow of 48.11 kg/s of AMP and 33.52 kg/s of PZ is required. A similar calculation for treating flue gas from syngas with 20.56 kg/s of CO₂ content shows that 67.17 kg/s of AMP and 46.8 kg/s of PZ are required. Under the proportion of 16% AMP and 14% PZ in aqueous solution, the required mass flow rate of lean AMP-PZ mixture solvent for treating 14.73 kg/s and 20.56 kg/s of CO₂ content in flue gases from methane and syngas fuel is calculated to be 137.68 kg/s and 192.22 kg/s respectively. As per the lean loading calculation, 8.79 kg-CO₂ and 3.43 kg-CO₂ are present in the total flow rate of 137.68 kg/s of solvent for treating flue gases from methane, which gives the lean amine used for the recirculation in PCCS process after regeneration of 14.88% AMP + 12.88% PZ + 4.5% CO₂ + 67.74% H₂O. The detailed parameters of the reference points of the streams in Fig. 4 of PCCS using AMP-PZ are given in Appendix B.

5.2.3. Results of carbon capture and PCCS power consumption

The MEA and AMP-PZ solvents with a similar CO₂ capture efficiency of 90% are used to treat the same amount of flue gas from methane and

Table 10
Parameters of flue gas from methane with and without PCCS.

Parameters	Unit	Without PCCS	With PCCS			
			Load conditions			
			100%	75%	50%	25%
Mass flow of flue gas at PCSS inlet	kg/ s	267.78	267.78	200.84	133.89	66.95
Mass flow of treated flue gas	kg/ s	–	254.52	190.89	127.26	63.63
CO ₂ captured	kg/ s	–	13.26	9.94	6.63	3.31
CO ₂ in fuel	kg/ s	–				

Table 11
Parameters of flue gas from syngas with and without PCCS.

Parameters	Unit	Without PCCS	With PCCS			
			Load conditions			
			100%	75%	50%	25%
Mass flow of flue gas at PCSS inlet	kg/ s	267.04	267.04	200.28	133.52	66.76
Mass flow of treated flue gas	kg/ s	–	248.53	186.4	124.27	62.13
CO ₂ captured	kg/ s	–	18.51	13.88	9.26	4.63
CO ₂ in fuel	kg/ s			8.92		

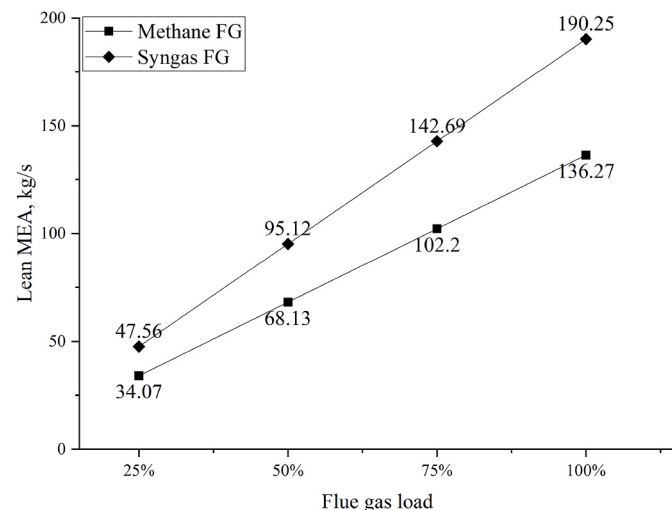


Fig. 11. Lean MEA mass flow at absorber inlet.

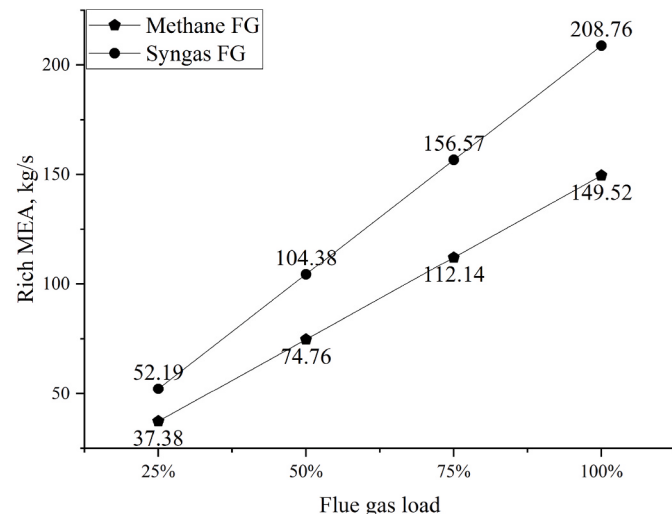


Fig. 12. Rich MEA at stripper inlet.

syngas at different load conditions with the same content are used for the analysis. Hence, the mass flow parameters of flue gases at different loads, captured and emitted CO₂ remain the same when using MEA and AMP-PZ for PCCS process as in Tables 10 and 11. When the flue gas load condition from CCGT exhaust to PCCS is reduced, the flue gas is diverted from the PCCS and passed directly into the atmosphere. The flue gases from methane and syngas passing through the PCCS at different load conditions are treated, 90% of CO₂ is captured, and the remaining CO₂ is

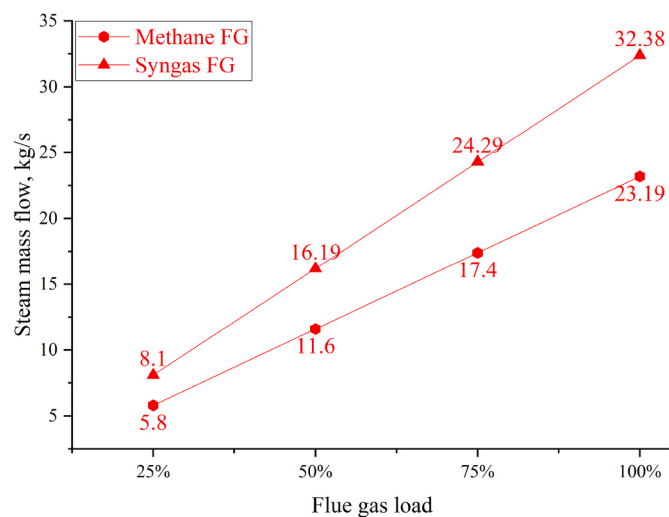


Fig. 13. Mass flow of steam consumed for MEA regeneration.

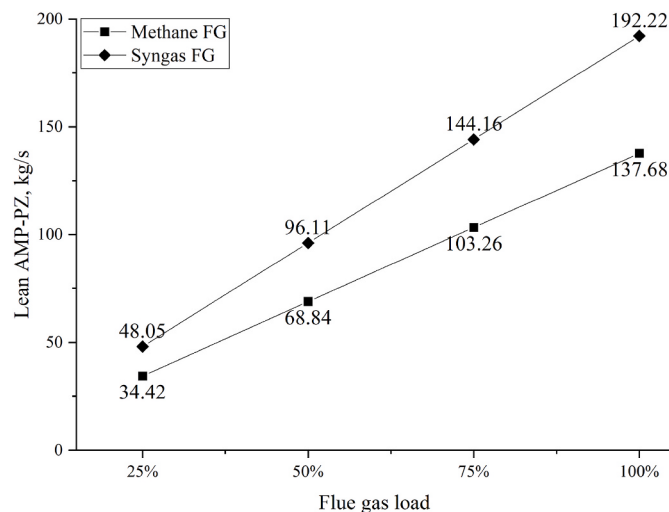


Fig. 14. Mass flow of lean AMP-PZ solvent at absorber inlet.

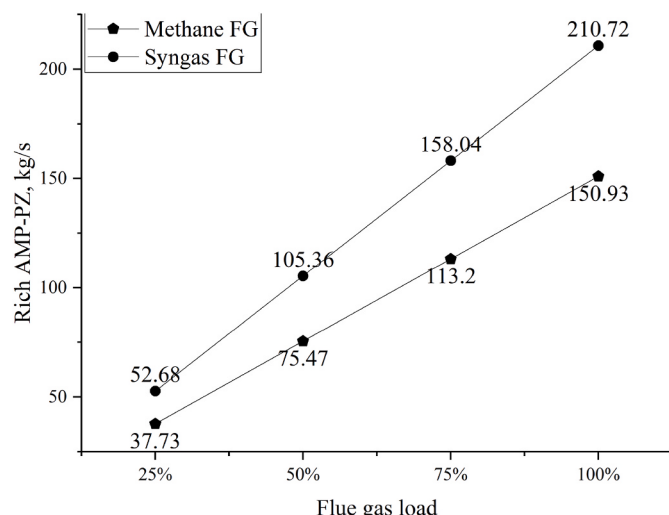


Fig. 15. Rich AMP-PZ mass flow at stripper inlet.

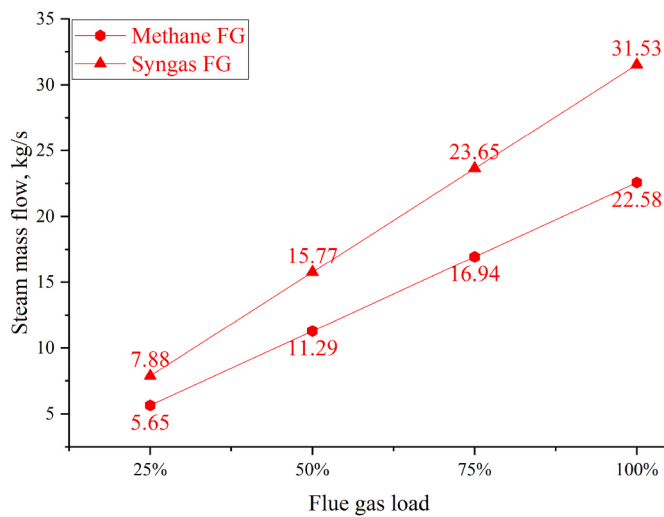


Fig. 16. Mass flow of steam consumed for AMP-PZ.

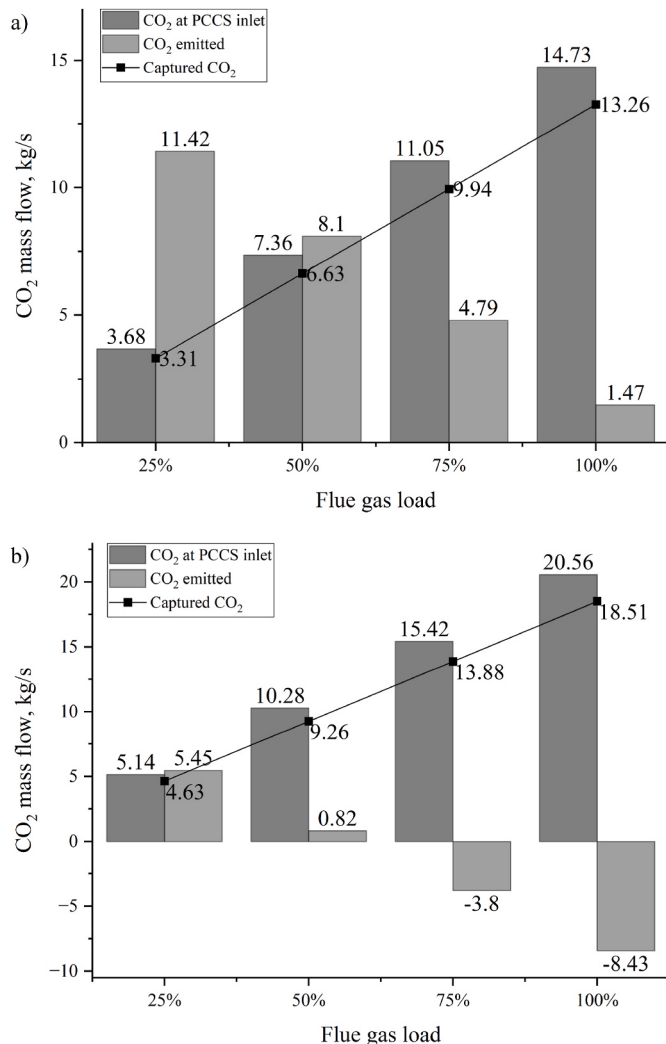


Fig. 17. Flue gases produced from a) methane and b) syngas treated with PCCS at different load conditions.

emitted, as in Fig. 17.

In Fig. 17(a) and (b), due to the capture efficiency of solvent, 90% of CO₂ is removed from the flue gas. The treated flue gas passed into the atmosphere consists of 10% of CO₂ content that cannot be completely removed, which is indicated as CO₂ emitted. In Fig. 17(b), apart from the CO₂ in fuel after syngas combustion, 90% of CO₂ is captured by PCCS. When the syngas is burned, the CO₂ emission can be estimated as the CO₂ content in the syngas fuel (59.31% mass fraction or 8.92 kg/s mass flow rate). The CO₂ generated level from the combustion of hydrocarbons in a gas turbine is treated as zero-emission because of biogas produced from biomass origin fuel. In Fig. 17(b) the CO₂ captured mass flow rate by PCCS is presented. When the exhaust gas flow rate directed to the PCCS exceeds 50%, it is possible to obtain the negative CO₂ emission for the proposed and assumed operating conditions, which is 100% and 75% of the flue gas produced from syngas directed to the PCCS to perform CO₂ capture process. The CO₂ in flue gas diverted from PCCS and the 10% flue gas from PCCS are considered to be negative emissions. At low 50% and 25% load conditions, a large amount of untreated flue gas at a mass flow rate of 133.52 kg/s and 200.28 kg/s is diverted from PCCS directly into the atmosphere.

The mass flow reduction of the streams in PCCS during different load conditions reduces the power consumed by PCCS, which reduces the total power consumption of PCCS as shown in Fig. 18.

Comparing the cases in Fig. 18, the CO₂ captured from syngas flue gas is high compared to methane, hence the power consumption for CO₂ compression is higher. The increase in CO₂ content in flue gas increases the flow rate of the solvent required for the PCCS process and flow rate of captured CO₂ at the final stage of the process, which needs more operation in the solvent pumps and CO₂ compressors. Hence, the power consumed by PCCS increases with an increase in CO₂ content in flue gas. It is necessary to increase the pressure of the flue gas from CCGT to the absorber operating condition of 1 bar. The blower and compressors of PCCS consume high power as shown in Fig. 19 for flue gas from methane and syngas. This is due to the high mass flow rate and pressure requirement of flue gas. As mentioned in Tables 10 and 11 for the various flue gas flow rate and captured CO₂, the blower increases the pressure of the flue gas to 1.15 bar and the CO₂ is compressed in various stages until it reaches the pressure of 110 bar for storage. The amine pumps and cooling water pumps consume 0.21 MW–0.05 MW of power from load conditions of 100%–25% respectively.

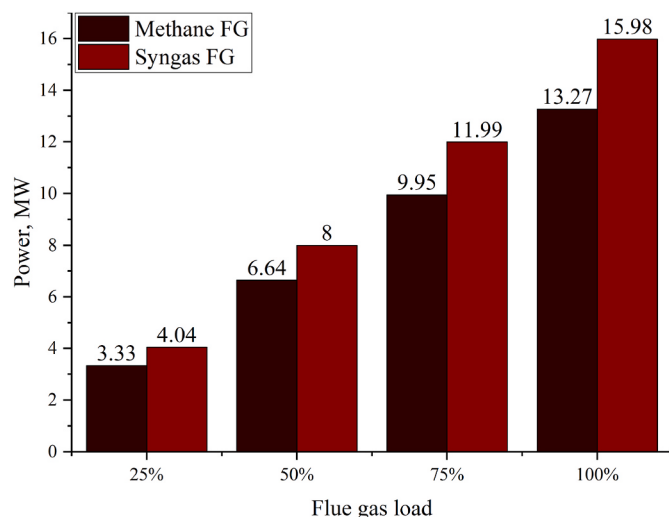


Fig. 18. Total power consumed by equipment in PCCS with flue gas from methane and syngas.

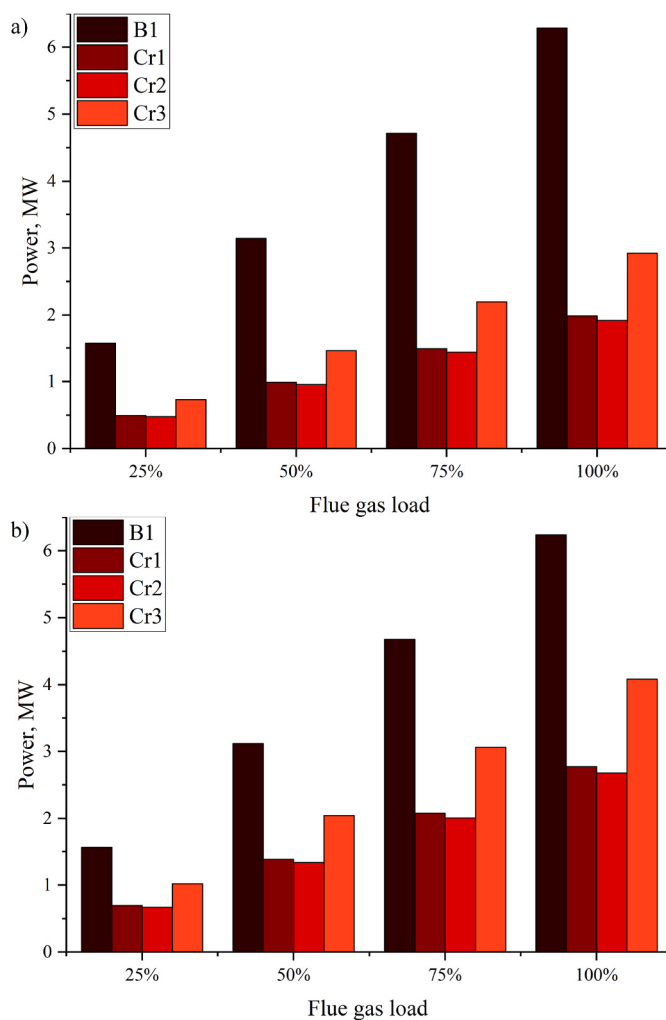


Fig. 19. Power consumed by blower and compressors in PCCS with flue gas from a) methane and b) syngas.

6. Conclusions

The analysis of heat recovery steam generator of a combined cycle power plant integrated with post-combustion carbon capture technology using solvent method is performed. Flue gases obtained from the combustion of methane and syngas of a gas turbine with CO₂ mass proportion of 5.44% and 7.7% respectively are used to calculate the enthalpy of flue gas, logarithmic mean temperature difference and heat exchange rate of components of one HRSG. From the obtained data, the temperature distribution and heat flow of one HRSG using flue gases from different fuels are plotted. The properties of the streams calculated in HRSG and the heat distribution in HRSG give a better understanding of the performance of HRSG. Even with the fixed stream temperature difference and pressure drop of the components, due to the mass flow and content of the flue gas, a slight difference in the enthalpy of flue gas, LMTD and heat rate of components of HRSG is observed.

The mass flow rate of flue gases from two HRSG at different load conditions is considered for the analysis of PCCS technology using MEA and AMP-PZ. The operating temperature and pressure of the absorber at 1 bar and 40 °C, and the stripper at 2 bar and 120 °C in PCCS are maintained the same using MEA and AMP-PZ solvents. However, the mass flow rate of solvents changes for MEA 136.27 kg/s and AMP-PZ 190.25 kg/s for treating flue gas from methane and MEA 137.68 kg/s and AMP-PZ 192.22 kg/s for treating flue gas from syngas. This is due to the rich CO₂ loading of the solvents. If the CO₂ loading of the solvents

differs, the mass flow of amine will increase or decrease. The lower rich CO₂ loading of amine increases the requirement of the mass flow rate of solvent for PCCS process and vice versa. The lean MEA and lean AMP-PZ, mass flow rate is higher when the syngas is used as the gas fuel compared to methane. However, the amount of lean and rich solvents is slightly higher when AMP-PZ is used for both fuels. This is due to the lean loading of AMP-PZ bit lower than MEA taken for consideration.

With the consideration of reboiler duty taken for MEA and AMP-PZ as 3.8 MJ/kg-CO₂ and 3.7 MJ/kg-CO₂. The mass flow rate of steam required by the reboiler for regenerating AMP-PZ is 22.58 kg/s and 31.53 kg/s and for regenerating MEA is 23.19 kg/s and 32.38 kg/s for treating flue gases from methane and syngas respectively. The amine after the regeneration process consists of some content of CO₂, which is 3.68% CO₂ in lean MEA and 4.5% CO₂ in lean AMP-PZ cannot be completely removed by the regeneration process or requires a high amount of heat to remove the CO₂ completely. The requirement of a high amount of heat for the regeneration process may increase the operational cost of the process. With reference to the CCGT data, at full load flue gas flow conditions the PCCS consumes 9.6%–11.6% of power from the CCGT power plant depending upon the flue gas and solvent used.

AMP-PZ maintains similar process parameters compared to that of MEA except with a lower regeneration rate and lower requirement of steam from CCGT. As referred in Refs. [40,46], from the steam consumed by AMP-PZ and MEA for reboiler duty, the flow rate of steam requirement for regeneration is lower in PCCS using AMP-PZ than MEA. The extraction of steam from the bleed of steam turbine for the amine regeneration has some possible impacts on the steam cycle. Since amine regeneration is inevitable in the PCCS process, the required steam taken from the power plant will reduce the power generation in the steam cycle, which affects the overall power output and the net efficiency of the power plant. The theoretical study of PCCS technology allows for performance evaluation and provides insight into the potential improvements of PCCS under different operating conditions. This analysis is a very crucial step for developing a PCCS model and measuring the performance of power plant when integrated with PCCS technology.

The analysis results confirm the possibility of obtaining the negative CO₂ emission level when the syngas fuel is used in CCGT. When the fuel, consisting of 100% of syngas is burned in gas turbines, slightly more than 50% of produced exhaust gases are directed to the PCCS installation, allowing it to reach a zero CO₂ emission level. All these important issues, a zero-emission level target, high power consumption by PCCS equipment, steam flow required by the reboiler, reduced power generation, and lower cycle efficiency, have to be taken into account in the design process of PCCS installation capacity and integration with the existed thermal power units.

CRediT authorship contribution statement

Navaneethan Subramanian: Conceptualization, Methodology, Formal analysis, Investigation, Writing – original draft, Writing-Reviewing and Editing, Visualization. **Pawel Madejski:** Conceptualization, Methodology, Validation, Formal analysis, Investigation, Writing – original draft, Writing-Reviewing and Editing.

Declaration of competing interest

The authors declare that they have no known competing financial interests or personal relationships that could have appeared to influence the work reported in this paper.

Data availability

Data will be made available on request.

Acknowledgements

The research leading to these results has received funding from the Norway Grants 2014–2021 via the National Center for Research and Development in Poland. Article has been prepared within the frame of

the project: “Negative CO₂ emission gas power plant” - NOR/POL-NORCCS/NEGATIVE-CO2-PP/0009/2019–00 which is co-financed by program “Applied research” under the Norwegian Financial Mechanisms 2014–2021 POLNOR CCS 2019 - Development of CO₂ capture solutions integrated in power and industry processes.

Nomenclature

$h_{fg@t}$	enthalpy of the flue gas at the target temperature, kJ/kg
h_{fi}	enthalpy of flue gas at the inlet of the heat exchanger, kJ/kg
h_{fo}	enthalpy of flue gas at the outlet of the heat exchanger, kJ/kg
h_i	enthalpy of the selected gas component, kJ/kg
h_{si}	enthalpy of steam at the inlet of the heat exchanger, kJ/kg
h_{so}	enthalpy of steam at the outlet of the heat exchanger, kJ/kg
h_{21}	enthalpy of steam at reboiler inlet, kJ/kg
h_{22}	enthalpy of steam at reboiler outlet, kJ/kg
i	gas component
LMTD	logarithmic mean temperature difference, °C
$\dot{m}_{cap,CO2}$	mass flow of CO ₂ captured, kg/s
\dot{m}_{fg}	mass flow rate of flue gas, kg/s
$\dot{m}_{fg,CO2}$	mass flow rate of CO ₂ in flue gas, kg/s
m_{gamine}	CO ₂ -rich loading, kg/kg
$\dot{m}_{lpsteam}$	mass flow rate of LP steam, kg/s
\dot{m}_{steam}	mass flow rate of steam, kg/s
\dot{m}_{vapour}	mass flow rate of vapour present at the outlet stream of stripper, kg/s
\dot{m}_2	mass flow of flue gas at the inlet of the absorber, kg/s
\dot{m}_3	mass flow of flue gas at absorber inlet, kg/s
\dot{m}_4	mass flow of treated flue gas at absorber outlet, kg/s
\dot{m}_9	mass flow of rich amine at absorber outlet, kg/s
\dot{m}_{14}	mass flow of lean solvent at absorber inlet, kg/s
\dot{m}_{15}	mass flow of rich solvent at stripper inlet, kg/s
\dot{m}_{17}	total mass flow of lean solvent at stripper outlet, kg/s
\dot{m}_{19}	amount of lean solvent required for CO ₂ capture, kg/s
\dot{m}_{22}	mass flow of captured CO ₂ with vapour at the outlet of the stripper, kg/s
\dot{m}_{23}	mass flow of CO ₂ vapour at the outlet of stripper kg/s
\dot{m}_{31}	mass flow of captured CO ₂ to storage, kg/s
\dot{Q}_{amine}	reboiler duty of the amine, kJ/kg CO ₂
\dot{Q}_{21}	reboiler duty required for the carbon capture process, MW
T_{ci}	temperature of cold stream inlet, °C
T_{co}	temperature of cold stream outlet, °C
T_{hi}	temperature of hot stream inlet, °C
T_{ho}	temperature of hot stream outlet, °C
X_i	mass fraction of the gas component, %

Appendix A

Table 12
Parameters of PCCS using MEA at each reference point in Fig. 4

Reference points	With Flue gas from methane			With Flue gas from syngas
	P (bar)	T (°C)	M (kg/s)	M (kg/s)
0	0.978	112.20	267.78	267.04
1	1.15	132.91	267.78	267.04
2	1.1	65.00	267.78	267.04
3	1.05	40	267.78	267.04
4	0.9	40.40	254.52	248.53
5	0.89	111.60	254.52	248.53
5a	0	0.00	0.00	0.00
5 b	0.89	111.60	254.52	248.53
5c	1.15	151	254.52	248.53
6	1	35	197.40	197.40
6a	1	15	Required	Required
6 b	1	35	197.40	197.40
7	1.1	35	197.40	197.40
8	1.05	30	197.40	197.40
9	0.9	60	149.52	208.76

(continued on next page)

Table 12 (continued)

Reference points	With Flue gas from methane			With Flue gas from syngas
	P (bar)	T (°C)	M (kg/s)	M (kg/s)
10	2.1	60	149.52	208.76
11	1.5	70	136.27	190.25
12	1	70	136.27	190.25
12a	1	30	Required	Required
12 b	1	30	Required	Required
13	1.05	70	136.27	190.25
14	1	40	136.27	190.25
15	2.05	100	149.52	208.76
16	1	120	121.32	169.37
17	1	115	136.27	190.25
18	1.55	115	136.27	190.25
19	2.03	120	149.52	208.76
20	2.01	125	149.52	208.76
21	3	135	23.19	32.38
22	2.9	132.37	23.19	32.38
23	1	120	28.21	39.38
24	0.95	30	24.47	34.16
25	0.95	30	3.74	5.22
26	3.8	150.00	24.47	34.16
27	3.75	30	20.73	28.94
28	15	150.00	20.73	28.94
29	14.95	30	16.99	23.72
30	110.5	209.00	16.99	23.72
31	110	22	13.26	18.51

Appendix B**Table 13**

Parameters of PCCS using AMP-PZ at each reference point in Fig. 4

Reference points	With Flue gas from methane			With Flue gas from syngas
	P (bar)	T (°C)	M (kg/s)	M (kg/s)
0	0.978	112.20	267.78	267.04
1	1.15	132.91	267.78	267.04
2	1.1	65.00	267.78	267.04
3	1.05	40	267.78	267.04
4	0.9	40.40	254.52	248.53
5	0.89	111.60	254.52	248.53
5a	0	0.00	0.00	0.00
5 b	0.89	111.60	254.52	248.53
5c	1.15	151	254.52	248.53
6	1	35	197.40	197.40
6a	1	15	Required	Required
6 b	1	35	197.40	197.40
7	1.1	35	197.40	197.40
8	1.05	30	197.40	197.40
9	0.9	60	150.93	210.72
10	2.1	60	150.93	210.72
11	1.5	70	137.67	192.21
12	1	70	137.68	192.22
12a	1	30	Required	Required
12 b	1	30	Required	Required
13	1.05	70	137.68	192.22
14	1	40	137.68	192.22
15	2.05	100	150.93	210.72
16	1	120	122.58	171.14
17	1	115	137.67	192.21
18	1.55	115	137.67	192.21
19	2.03	120	150.93	210.72
20	2.01	125	150.93	210.72
21	3	135	22.58	31.53
22	2.9	132.37	22.58	31.53
23	1	120	28.35	39.58
24	0.95	30	24.58	34.31
25	0.95	30	3.77	5.27
26	3.8	150.00	24.58	34.31
27	3.75	30	20.80	39.04
28	15	150.00	20.80	39.04
29	14.95	30	17.03	23.77
30	110.5	209.00	17.03	23.77
31	110	22	13.26	18.51

References

- [1] Sifat NS, Haseli Y. A critical review of CO₂ capture technologies and prospects for clean power generation. *Energies* 2019;12(21). <https://doi.org/10.3390/en12214143>. MDPI AG.
- [2] Hamilton I, et al. The public health implications of the Paris Agreement: a modelling study. *Lancet Planet Health* Feb. 2021;5(2):e74–83. [https://doi.org/10.1016/S2542-5196\(20\)30249-7](https://doi.org/10.1016/S2542-5196(20)30249-7).
- [3] Peridas G, Mordick Schmidt B. The role of carbon capture and storage in the race to carbon neutrality. *Electr J Aug.* 2021;34(7). <https://doi.org/10.1016/j.tej.2021.106996>.
- [4] de Kleijne K, Hanssen SV, van Dinteren L, Huijbregts MAJ, van Zelm R, de Coninck H. Limits to Paris compatibility of CO₂ capture and utilization. *One Earth* Feb. 2022;5(2):168–85. <https://doi.org/10.1016/j.oneear.2022.01.006>.
- [5] Bajpai S, et al. Opportunities, challenges and the way ahead for carbon capture, utilization and sequestration (CCUS) by the hydrocarbon industry: towards a sustainable future. *Energy Rep Nov.* 2022;8:15595–616. <https://doi.org/10.1016/j.egyr.2022.11.023>.
- [6] IEA. Carbon capture, utilisation and storage". Paris: IEA; 2022. <https://www.iea.org/reports/carbon-capture-utilisation-and-storage-2>. License: CC BY 4.0.
- [7] IEA GREENHOUSE GAS R&D PROGRAMME towards zero emissions CCS in power plants using higher capture rates or biomass [Online]. Available: www.ieaghg.org; 2019.
- [8] IEA. Is carbon capture too expensive? Paris: IEA; 2021. <https://www.iea.org/commentaries/is-carbon-capture-too-expensive>.
- [9] Cherepovitsyna A, Kuznetsova E, Guseva T. The costs of CC(U)S adaptation: the case of Russian power industry. *Energy Rep Mar.* 2023;9:704–10. <https://doi.org/10.1016/j.egyr.2022.11.104>.
- [10] Mantripragada HC, Zhai H, Rubin ES. Boundary Dam or Petra Nova – which is a better model for CCS energy supply? *Int J Greenh Gas Control* Mar. 2019;82:59–68. <https://doi.org/10.1016/j.ijggc.2019.01.004>.
- [11] Stéphenne K. Start-up of world's first commercial post-combustion coal fired CCS project: contribution of shell cansolv to SaskPower boundary dam ICCS project. *Energy Proc* 2014;63:6106–10. <https://doi.org/10.1016/j.egypro.2014.11.642>.
- [12] Shell Global, "<https://www.shell.com/business-customers/catalysts-technologies/resources-library/trade-release-shell-catalysts-and-technologies-and-calpine-deer-park-energy-center.html>" 2021. (Last visited: 16/03/2023).
- [13] Kotowicz J, Brzczek M. Analysis of increasing efficiency of modern combined cycle power plant: a case study. *Energy Jun.* 2018;153:90–9. <https://doi.org/10.1016/j.energy.2018.04.030>.
- [14] Bianco N, Fragnito A, Iasiello M, Maria Mauro G. A comprehensive approach for the multi-objective optimization of Heat Recovery Steam Generators to maximize cost-effectiveness and output power. *Sustain Energy Technol Assessments Jun.* 2021;45:101162. <https://doi.org/10.1016/j.seta.2021.101162>.
- [15] Gou X, Zhang H, Li G, Cao Y, Zhang Q. Dynamic simulation of a gas turbine for heat recovery at varying load and environment conditions. *Appl Therm Eng* 2021; 117014. <https://doi.org/10.1016/j.applthermaleng.2021.117014>.
- [16] Madejski P, Zymekla P, Wozik RW, Kubicek H. Gas fired plant modeling for monitoring and optimization of electricity and heat production. *Journal of Power Technologies* 2017;97(5):455–62. 2017.
- [17] Shin JY, Jeon YJ, Maeng DJ, Kim JS, Ro ST. Analysis of the dynamic characteristics of a combined-cycle power plant. *Energy* 2002;27(12):1085–98. [https://doi.org/10.1016/S0360-5442\(02\)00087-7](https://doi.org/10.1016/S0360-5442(02)00087-7).
- [18] IEA. Bioenergy with carbon capture and storage. Paris: IEA; 2022. <https://www.iea.org/reports/bioenergy-with-carbon-capture-and-storage>. License: CC BY 4.0.
- [19] Ma C, et al. Towards negative carbon emissions: carbon capture in bio-syngas from gasification by aqueous pentaethylenehexamine. *Appl Energy Dec.* 2020;279: 115877. <https://doi.org/10.1016/j.apenergy.2020.115877>.
- [20] Ronda A, Haro P, Gómez-Barea A. Sustainability assessment of alternative waste-to-energy technologies for the management of sewage sludge. *Waste Manag Mar.* 2023;159:52–62. <https://doi.org/10.1016/j.wasman.2023.01.025>.
- [21] Vishwajeet, et al. Entrained flow plasma gasification of sewage sludge—proof-of-concept and fate of inorganics. *Energies Mar.* 2022;15(5):1948. <https://doi.org/10.3390/en15051948>.
- [22] Ziolkowski P, et al. Thermodynamic analysis of negative CO₂ emission power plant using aspen Plus. Aspen Hysys, and Epsilon Software", *Energies (Basel)* Oct. 2021; 14(19):6304. <https://doi.org/10.3390/en14196304>.
- [23] Madejski P, Chmiel K, Subramanian N, Kuś T. Methods and techniques for CO₂ capture: review of potential solutions and applications in modern energy technologies. *Energies* 2022;15(3). <https://doi.org/10.3390/en15030887>. MDPI, Feb. 01.
- [24] el Hadri N, Quang DV, Goetheer ELV, Abu Zahra MRM. Aqueous amine solution characterization for post-combustion CO₂ capture process. *Appl Energy* Jan. 2017; 185:1433–49. <https://doi.org/10.1016/j.apenergy.2016.03.043>.
- [25] Kim S, et al. Sustainable energy harvesting from post-combustion CO₂ capture using amine-functionalized solvents. *Energy Mar.* 2023;267:126532. <https://doi.org/10.1016/j.energy.2022.126532>.
- [26] He X, He H, Barzaghi F, Amer MW, Li C, Zhang R. Analysis of the energy consumption in solvent regeneration processes using binary amine blends for CO₂ capture. *Energy May* 2023;270:126903. <https://doi.org/10.1016/j.energy.2023.126903>.
- [27] He X, He H, Barzaghi F, Amer MW, Li C, Zhang R. Analysis of the energy consumption in solvent regeneration processes using binary amine blends for CO₂ capture. *Energy May* 2023;270:126903. <https://doi.org/10.1016/j.energy.2023.126903>.
- [28] Sakwattanapong R, Aroonwilas A, Veawab A. Behavior of reboiler heat duty for CO₂ capture plants using regenerable single and blended alkanolamines. *Ind Eng Chem Res Jun.* 2005;44(12):4465–73. <https://doi.org/10.1021/ie050063w>.
- [29] Śpiewak D, et al. PDU-Scale Experimental results of CO₂ removal with AMP/PZ Solvent. *Chem Process Eng Mar.* 2015;36(1):39–48. <https://doi.org/10.1515/cpe-2015-0003>.
- [30] van der Spek M, Arendsen R, Ramirez A, Faaij A. Model development and process simulation of postcombustion carbon capture technology with aqueous AMP/PZ solvent. *Int J Greenh Gas Control Apr.* 2016;47:176–99. <https://doi.org/10.1016/j.ijggc.2016.01.021>.
- [31] Spietz T, Dobras S, Chwola T, Wilk A, Krótki A, Więsław-Solny L. Experimental results of amine emission from the CO₂ capture process using 2-amino-2-methyl-1-propanol (AMP) with piperazine (PZ). *Int J Greenh Gas Control Nov.* 2020;102: 103155. <https://doi.org/10.1016/j.ijggc.2020.103155>.
- [32] Moser P, Wiechers G, Schmidl S, Veronezi Figueiredo R, Skylogianni E, Garcia Moret-Sohn Monteiro J. Conclusions from 3 years of continuous capture plant operation without exchange of the AMP/PZ-based solvent at Niederaussem – insights into solvent degradation management. *Int J Greenh Gas Control Jun.* 2023; 126:103894. <https://doi.org/10.1016/j.ijggc.2023.103894>.
- [33] Lisiecka K. Elektrociepłownia Gorzów pełna dobrej energii. PGE GiEK S.A. Oddział Elektrociepłownia Gorzów; 2017.
- [34] Siemens AG. SGT-800 gas turbine. 2013. <https://refman.energytransitionmodel.com/publications/1954/download>. Last visited: 01/07/2022.
- [35] Siemens AG. SST-400 industrial steam turbines. 2011. <https://www.hgpauction.com/wp-content/uploads/2014/01/Siemens-Industrial-Steam-Turbine-SST-400-Brochure.pdf>. Last visited: 01/07/2022.
- [36] Woudstra N, Woudstra T, Pirone A, van der Stelt T. Thermodynamic evaluation of combined cycle plants. *Energy Convers Manag* May 2010;51(5):1099–110. <https://doi.org/10.1016/j.enconman.2009.12.016>.
- [37] Elhosseini MA, shams El-din A, Ali HA, Abraham A. Heat recovery steam generator (HRSG) three-element drum level control utilizing Fractional order PID and fuzzy controllers. *ISA Trans Mar.* 2022;122:281–93. <https://doi.org/10.1016/j.isatra.2021.04.035>.
- [38] Jordán PS, et al. Techno-economic analysis of solar-assisted post-combustion carbon capture to a pilot cogeneration system in Mexico. *Energy Jan.* 2019;167: 1107–19. <https://doi.org/10.1016/j.energy.2018.11.010>.
- [39] Cecarelli N, et al. Flexibility of low-CO₂ gas power plants: integration of the CO₂ capture unit with CCGT operation. *Energy Proc* 2014;63:1703–26. <https://doi.org/10.1016/j.egypro.2014.11.179>.
- [40] S. Hume, P. Alto, S. A. Hume, M. I. Shah, G. Lombardo, and E. R. Kleppe, "Results from CESAR-1 testing with combined heat and power (CHP) flue gas at the CO₂ technology centre MONGSTAD".
- [41] Gorset O, Knudsen JN, Bade OM, Askestad I. Results from testing of aker solutions advanced amine solvents at CO₂ technology Centre mongstad. *Energy Proc* 2014; 63:6267–80. <https://doi.org/10.1016/j.egypro.2014.11.658>.
- [42] Choi WJ, Seo JB, Jang SY, Jung JH, Oh KJ. Removal characteristics of CO₂ using aqueous MEA/AMP solutions in the absorption and regeneration process" *Journal of Environ Sci J Integr Environ Res* 2009;21(7):907–13. [https://doi.org/10.1016/S1001-0742\(08\)62360-8](https://doi.org/10.1016/S1001-0742(08)62360-8).
- [43] Huertas JI, Gomez MD, Giraldo N, Garzón J. CO₂ absorbing capacity of MEA. *J Chem* 2015;2015:1–7. <https://doi.org/10.1155/2015/965015>.
- [44] Luis P. Use of monoethanolamine (MEA) for CO₂ capture in a global scenario: consequences and alternatives. *Desalination Feb.* 2016;380:93–9. <https://doi.org/10.1016/j.desal.2015.08.004>.
- [45] Xue B, Yu Y, Chen J, Luo X, Wang M. A comparative study of MEA and DEA for post-combustion CO₂ capture with different process configurations. *Int J Coal Sci Technol Mar.* 2017;4(1):15–24. <https://doi.org/10.1007/s40789-016-0149-7>.
- [46] Kachko A, et al. Real-time process monitoring of CO₂ capture by aqueous AMP-PZ using chemometrics: pilot plant demonstration. *Ind Eng Chem Res Jun.* 2015;54(21):5769–76. <https://doi.org/10.1021/acs.iecr.5b00691>.
- [47] Li Z, Chen S, Hopkinson D, Luebke D. Verification of a solvent optimization approach for post-combustion CO₂ capture using commercial alkanolamines. *Int J Greenh Gas Control Jan.* 2016;44:59–65. <https://doi.org/10.1016/j.ijggc.2015.11.002>.
- [48] Li S, Li H, Yu Y, Chen J. Simulation and performance comparison for CO₂ capture by aqueous solvents of N-(2-Hydroxyethyl) piperazine and another five single amines. *Processes Dec.* 2021;9(12):2184. <https://doi.org/10.3390/pr9122184>.
- [49] Dash SK, Samanta AN, Bandyopadhyay SS. Simulation and parametric study of post combustion CO₂ capture process using (AMP+PZ) blended solvent. *Int J Greenh Gas Control Feb.* 2014;21:130–9. <https://doi.org/10.1016/j.ijggc.2013.12.003>.
- [50] Porter RTJ, Fairweather M, Pourkashanian M, Woolley RM. The range and level of impurities in CO₂ streams from different carbon capture sources. *Int J Greenh Gas Control May* 2015;36:161–74. <https://doi.org/10.1016/j.ijggc.2015.02.016>.
- [51] Feron PHM, Cousins A, Jiang K, Zhai R, Garcia M. An update of the benchmark post-combustion CO₂-capture technology. *Fuel* 2020;273(Aug). <https://doi.org/10.1016/j.fuel.2020.117776>.
- [52] Jung J, Jeong YS, Lim Y, Lee CS, Han C. Advanced CO₂ capture process using MEA scrubbing: configuration of a split flow and phase separation heat exchanger. *Energy Proc* 2013;37:1778–84. <https://doi.org/10.1016/j.egypro.2013.06.054>.
- [53] J. Andersson, "An investigation of carbon capture technologies for Sävenäs waste-to-energy plant".
- [54] Morgan JC, et al. Development of a framework for sequential Bayesian design of experiments: application to a pilot-scale solvent-based CO₂ capture process. *Appl Energy* Mar. 2020;262:114533. <https://doi.org/10.1016/j.apenergy.2020.114533>.

- [55] Hasan S, Abbas AJ, Nasr GG. Improving the carbon capture efficiency for gas power plants through amine-based absorbents. *Sustainability* Dec. 2020;13(1):72. <https://doi.org/10.3390/su13010072>.
- [56] Oexmann J, Kather A. Post-combustion CO₂ capture in coal-fired power plants: comparison of integrated chemical absorption processes with piperazine promoted potassium carbonate and MEA. *Energy Proc* Feb. 2009;1(1):799–806. <https://doi.org/10.1016/j.egypro.2009.01.106>.
- [57] Çengel YAB, Kanoglu Michael A, Mehmet. *Thermodynamics - an engineering approach*, ninth ed. 2019.
- [58] NIST Chemistry WebBook, “<https://webbook.nist.gov/chemistry/>.” (Last visited: 11/03/2023).